Fractional-order position control for the fully-actuated Hexa-rotor: SITL simulations in the PX4 firmware
Supplementary material

Andrés Montes de Oca, Alejandro Flores, and Gerardo Flores*, *Member, IEEE*

I. Simulations

A. MATLAB Simulink numerical simulations

In this subsection, we detail the results obtained from numerical simulations using MATLAB Simulink. To compute the fractional-order integral in the position control, we used the FOMCON toolbox [1], which provides a variety of fractional-order differintegral blocks for control applications. We also simulated the PID control algorithm for comparison purposes.

The control allocation problem is solved from the control inputs in u_τ and μ through the following expression [2],

$$\begin{bmatrix} \mu \\ u_\tau \end{bmatrix} = B(\alpha_i, \beta_i, \lambda, l)\mathrm{v}, \tag{1}$$

where $\mathrm{v} = \left[\omega_1^2, \omega_2^2, ..., \omega_6^2\right]^\intercal$ is the motor spinning rate vector and ω_i is the angular velocity of the i-th motor. $B(\cdot)$ is a function that depends on the Hexa-rotor's parameters such as tilting angles (β, α), motor's arm length l, and distance between motors λ.

TABLE I: Parameter values used in the MATLAB simulation.

$g = 9.81$	$\alpha = -0.5$	$k_3 = \mathrm{diag}[30\ 30\ 30]$
$m = 1$	$\Lambda = \mathrm{diag}[7\ 7\ 7]$	$k_4 = \mathrm{diag}[10\ 10\ 10]$
$\hat{e}_3 = [0\ 0\ 1]$	$K_1 = \mathrm{diag}[50\ 50\ 50]$	$k_R = \mathrm{diag}[50\ 50\ 50]$
$J = \mathrm{diag}([1\ 1\ 1])$	$K_2 = \mathrm{diag}[10\ 10\ 10]$	$k_\Omega = \mathrm{diag}[10\ 10\ 10]$
$K_p = \mathrm{diag}[70\ 70\ 70]$	$K_d = \mathrm{diag}[20\ 20\ 20]$	$K_i = \mathrm{diag}[1\ 1\ 1]$

For the simulations, we used the parameter listed in Table I. The results obtained from the simulations are shown in Figs. 1, 2, and 3. First, we show the behavior of the UAV position states during the flight envelope in Fig. 1. This figure depicts the position response under a PID control and the fractional-order control using four different integration orders $I^{0.25}, I^{0.5}, I^{0.75}$. Using the PID control, the errors are considerably bigger than the fractional-order control, reaching error values around ± 0.5 meters. For the case of the fractional-order control, we can see that the errors are smaller with maximum error values around ± 0.05 meters. Now in Fig. 2 we depict the attitude states. It can be seen that the states converge to zero with no oscillation for all the controls. This means that the proposed position control does not affect attitude stability. Finally, the position control outputs are plotted in Fig. 3, where one can see the continuity and smoothness of the signals.

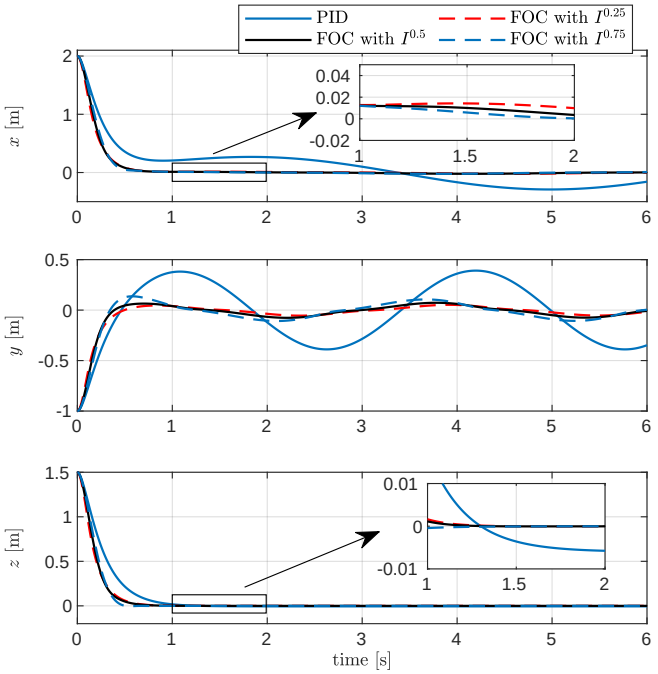

Fig. 1: Position obtained in different simulations varying the fractional-order integration and comparing to the common PID control approach.

B. SITL simulations

This subsection presents the results obtained from the SITL simulations using a virtual environment in Gazebo and the PX4 firmware. The proposed fractional-order control is implemented in the original code using the parameters listed in Table II.

A. Montes de Oca, A. Flores, and G. Flores are with the Laboratorio de Percepción y Robótica (LAPyR), Center for Research in Optics, Loma del Bosque 115, León, Guanajuato, 37150 Mexico. (e-mails: andresmr@cio.mx, alejandrofl@cio.mx, and gflores@cio.mx, *corresponding author.)

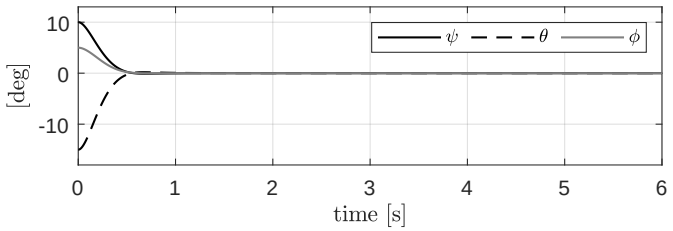

Fig. 2: Attitude states obtained in simulation applying the proposed control approach with fractional-order integration $\alpha = 0.25$.

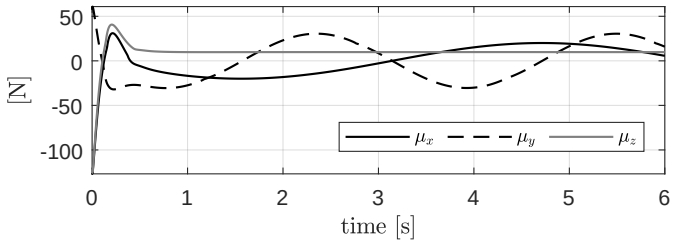

Fig. 3: The proposed fractional-order position control with $\alpha = 0.25$.

Fig. 4 depicts the position states of the multi-rotor while following a circular-shaped trajectory described by

$$\begin{aligned} x_d(t) &= 4\sin 0.1t, \\ y_d(t) &= 4\cos 0.1t, \\ z_d(t) &= 7.5. \end{aligned} \tag{2}$$

Adding these functions as disturbances to the system makes it easy to observe that the proposed control presents a better performance compared to the conventional PID. From the

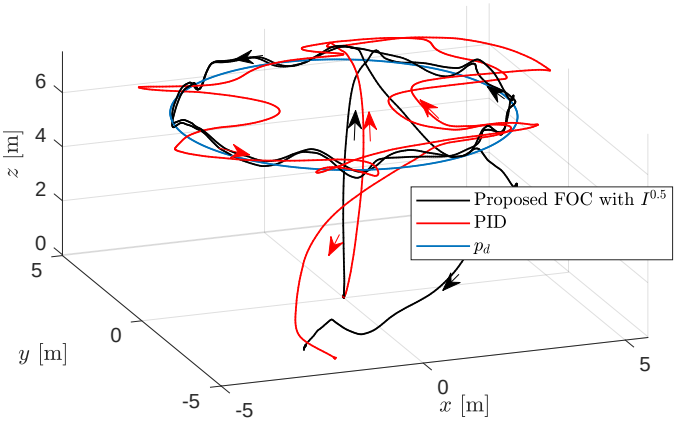

Fig. 4: Position obtained during a SITL simulation performing a circular path tracking between the proposed fractional-order control and the standard PID control approach. The disturbances added to this simulation are defined in (2).

same simulation, position errors with the proposed control are depicted in Fig. 5. Since this work's main contribution relies on position control, we only present the attitude results for the fractional-order control simulation to prove that the fully actuated Hexa-rotor does not require to modify its orientation

TABLE II: Parameter values used in the SITL simulation.

$g = 9.81$	$\alpha = -0.5$	$k_3 = \text{diag}[0.2\ 0.2\ 0.2]$
$m = 2.02$	$\Lambda = \text{diag}[1\ 1\ 1]$	$k_4 = \text{diag}[0.01\ 0.01\ 0.01]$
$\hat{e}_3 = [0\ 0\ 1]$	$K_1 = \text{diag}[10\ 10\ 10]$	$k_R = \text{diag}[0.2\ 0.2\ 0.2]$
$J = \text{diag}([0.011\ 0.015\ 0.021])$	$K_2 = \text{diag}[10\ 10\ 10]$	$k_\Omega = \text{diag}[0.06\ 0.06\ 0.06]$
$K_p = \text{diag}[70\ 70\ 70]$	$K_d = \text{diag}[20\ 20\ 20]$	$K_i = \text{diag}[1\ 1\ 1]$

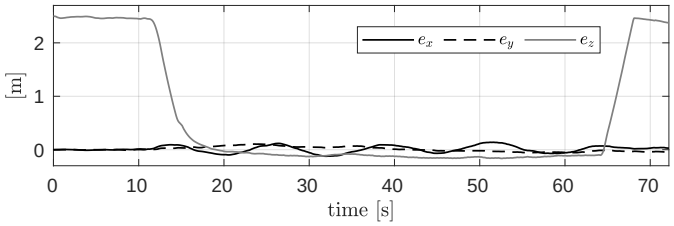

Fig. 5: Hexa-rotor's position errors during the SITL simulation with the fractional-order control and under exogenous disturbances.

to perform position commands. This is shown in Fig. 6, where the roll and pitch angles remain low, with values close to zero during the disturbance rejection.

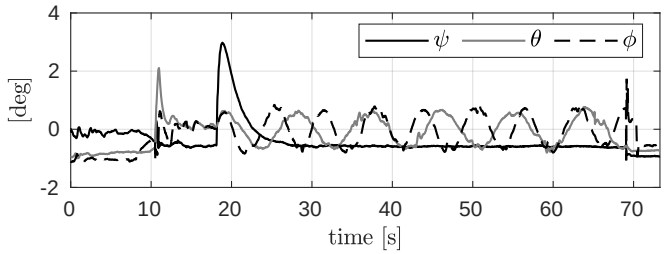

Fig. 6: Hexa-rotor's attitude states during the SITL simulation. It can be seen that the attitude is maintained close to zero regardless of the position control commands. This is possible thanks to the full actuation of the Hexa-rotor.

Additionally, we conduct a performance comparison between different fractional-order values of α in a positioning SITL simulation. In Fig. 7 it is shown the 3D plots of the flights under the FOC with $\alpha = 0.25, 0.5, 0.75$. In the three flight simulations, it is observed that the response is similar with small errors. For better visualization, we depict the position states (x, y, z) for the three FOC simulations in separate plots in Fig. 8. In this case, it is easier to see that flight performed using $\alpha = 0.75$ performs the worst from the three simulations while using $\alpha = 0.25$ performs the best.

Finally, we aim to demonstrate that the use of $\dot{p}_d$ and $\ddot{p}_d$ in the control law reduces the error and noise in the path tracking. For that reason, we performed a SITL simulation comparison between the implementation of these terms and without them. The results can be seen in Fig. 9. In this figure, we depict the position states (x, y) response in two cases: a) using only x_d and b) using $x_d, \dot{p}_d, \ddot{p}_d$. It can be seen that for the second case, the position states are less noisy and close to the reference.

REFERENCES

[1] A. Tepljakov, E. Petlenkov, and J. Belikov, "Fomcon: Fractional-order modeling and control toolbox for matlab," in *Proceedings of the 18th In-*

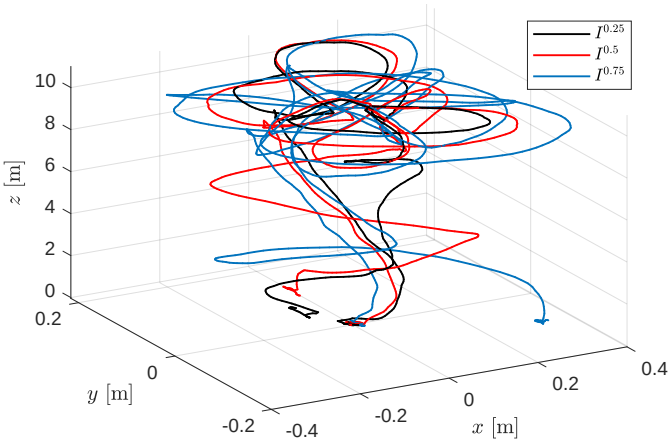

Fig. 7: 3D position obtained during a SITL simulation performing positioning task using three different fractional order values.

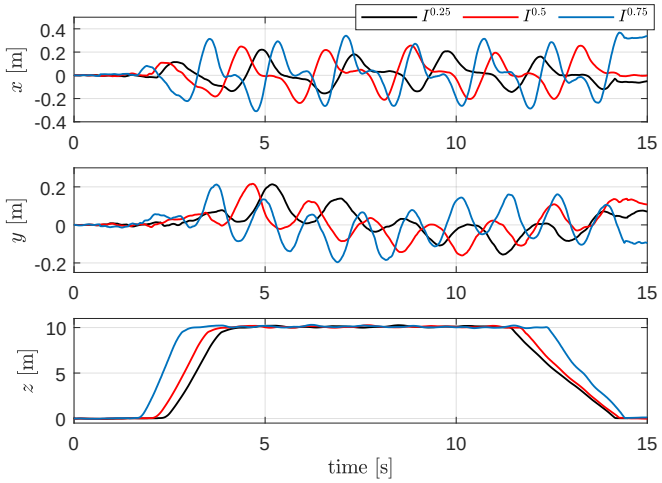

Fig. 8: Axis position obtained during SITL simulations with three different fractional order values.

ternational Conference Mixed Design of Integrated Circuits and Systems - MIXDES 2011, 2011, pp. 684–689.

[2] G. Flores, A. M. de Oca, and A. Flores, "Robust nonlinear control for the fully actuated hexa-rotor: Theory and experiments," *IEEE Control Systems Letters*, vol. 7, pp. 277–282, 2023.

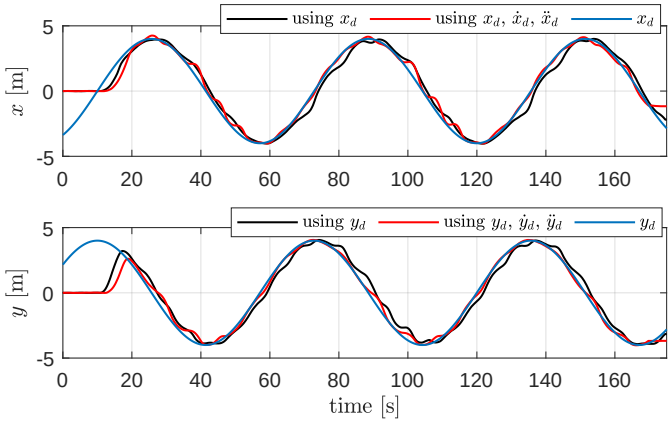

Fig. 9: Path tracking results showing the importance of using $\dot{p}_d$ and $\ddot{p}_d$ terms in the control law.